Harmful Algae 104 (2021) 102031

Contents lists available at ScienceDirect

Harmful Algae

journal homepage: www.elsevier.com/locate/hal

Original Article

Transcriptomic and isotopic data reveal central role of ammonium in facilitating the growth of the mixotrophic dinoflagellate, *Dinophysis acuminata*

Theresa K. Hattenrath-Lehmann [a,1,2], Deepak Nanjappa [a,1], Huan Zhang [b,1], Liying Yu [c], Jennifer A. Goleski [a], Senjie Lin [b,c], Christopher J. Gobler [a,*]

[a] Stony Brook University, School of Marine and Atmospheric Sciences, 239 Montauk Hwy, Southampton, NY 11968, United States
[b] Department of Marine Sciences, University of Connecticut, Groton, CT 06340, United States
[c] State Key Laboratory of Marine Environmental Science and Marine Biodiversity and Global Change Research Center, Xiamen University, Xiamen 361101, China

ARTICLE INFO

Keywords:
Dinophysis
Nitrate
Ammonium
Transcriptome
N-15

ABSTRACT

Dinophysis spp. are mixotrophs that are dependent on specific prey, but are also potentially reliant on dissolved nutrients. The extent to which *Dinophysis* relies on exogenous N and the specific biochemical pathways important for supporting its autotrophic and heterotrophic growth are unknown. Here, the nutritional ecology of *Dinophysis* was explored using two approaches: 1) ^{15}N tracer experiments were conducted to quantify the concentration-dependent uptake rates and associated kinetics of various N compounds (nitrate, ammonium, urea) of *Dinophysis* cultures and 2) the transcriptomic responses of *Dinophysis* cultures grown with multiple combinations of prey and nutrients were assessed via dinoflagellate spliced leader-based transcriptome profiling. Of the N compounds examined, ammonium had the highest V_{max} and affinity coefficient, and lowest K_s for both pre-starved and pre-fed cultures, collectively demonstrating the preference of *Dinophysis* for this N source while little-to-no nitrate uptake was observed. During the transcriptome experiments, *Dinophysis* grown with nitrate and without prey had the largest number of genes with lower transcript abundances, did not increase abundance of transcripts associated with nitrate/nitrite uptake or reduction, and displayed no cellular growth, suggesting *D. acuminata* is not capable of growing on nitrate. When offered prey, the transcriptomic response of *Dinophysis* included the production of phagolysosomes, enzymes involved in protein and lipid catabolism, and N acquisition through amino acid degradation pathways. Compared with cultures only offered ammonium or prey, cultures offered both ammonium and prey had the largest number of genes with increased transcript abundances, the highest growth rate, and the unique activation of multiple pathways involved in cellular catabolism, further evidencing the ability of *Dinophysis* to grow optimally as a mixotroph. Collectively, this study evidences the key role ammonium plays in the mixotrophic growth of *Dinophysis* and reveals the precise biochemical pathways that facilitate its mixotrophic growth.

1. Introduction

In recent decades, harmful algal blooms have increased in frequency, intensity and range, and have become a global-scale concern due to their potential economic, environmental and human health impacts (Anderson et al., 2012; Glibert et al., 2005; Hallegraeff, 2010). While diarrhetic shellfish poisoning (DSP) caused by the toxin-producing (okadaic acid and dinophysistoxins) dinoflagellates of the genus *Dinophysis* has been a common occurrence in Europe, Asia and South America for decades (Hallegraeff, 1993; Van Dolah, 2000), it has only recently emerged in the United States (Reguera et al., 2014, 2012). During the last decade, there have been numerous reports of DSP toxin levels in shellfish exceeding the FDA action limit (160 ng g^{-1} of shellfish tissue) on multiple US coastlines, including the West (Lloyd et al., 2013; Peacock et al., 2018; Shultz et al., 2019; Trainer et al., 2013), East (DMF, 2015; Hattenrath-Lehmann et al., 2018, 2013; Wolny et al., 2020) and Gulf coasts

* Corresponding author.
E-mail address: christopher.gobler@stonybrook.edu (C.J. Gobler).
[1] The authors contributed equally.
[2] Current address: Wadsworth Center, New York State Department of Health, Empire Plaza, Albany, New York, 12223, USA

https://doi.org/10.1016/j.hal.2021.102031
Received 1 January 2021; Received in revised form 8 April 2021; Accepted 9 April 2021
Available online 27 April 2021

(Campbell et al., 2010; Deeds et al., 2010; Swanson et al., 2010). While anthropogenic nutrient loading has, in many cases, been cited as a main contributing factor to the persistence and expansion of several HABs (Anderson et al., 2008; Heisler et al., 2008), the role of nutrients in the occurrence of *Dinophysis* blooms is poorly understood.

The ability to culture *Dinophysis* (Park et al., 2006) has greatly expanded the understanding of multiple facets of its ecology. Traditionally, nitrogenous nutrients were considered to play little role, if any, in the ecology of *Dinophysis* given that cultures were not able to be established using traditional nutrient media (Maestrini et al., 1995; Reguera et al., 2012; Sampayo, 1993) but rather required the addition of live prey, specifically the ciliate *Mesodinium rubrum* (Park et al., 2006). More recent research, however, has demonstrated that cultures (Hattenrath-Lehmann and Gobler, 2015) and field populations (Hattenrath-Lehmann et al., 2015) of *Dinophysis* from NY, USA, are capable of using various organic and inorganic nitrogenous nutrients to significantly increase its growth rate and in some cases, can acquire the majority of its cellular N demand from dissolved nutrients (Hattenrath-Lehmann and Gobler, 2015). While the ability of *Dinophysis* to assimilate nutrients has been affirmed via ^{15}N uptake experiments (Hattenrath-Lehmann and Gobler, 2015; García-Portela et al., 2020), concentration-dependent N uptake rates and the specific pathways important for supporting autotrophic and heterotrophic growth in this mixotroph are largely unknown.

During the past few decades, molecular methods such as qPCR, dPCR, microrrays, in situ hybridization assays, and high throughput amplicon sequencing have been instrumental in HAB monitoring efforts (Medlin, 2013; Medlin and Orozco, 2017), while metagenomics, transcriptomics and proteomics have been used to enhance our understanding of HAB ecology (Anderson et al., 2012; Bi et al., 2019; Cooper et al., 2014; Kudela et al., 2010b; Zhang et al., 2019; Zhuang et al., 2015). Experiments targeting specific conditions in combination with transcriptomics have been pivotal in identifying genes responsible for regulating certain physiological processes of HABs (Harke and Gobler, 2015; Kudela et al., 2010b; Wurch et al., 2019). Molecular studies involving assessing the genomes and/or transcriptomes of dinoflagellates have been challenging due to large genomes, sequence redundancy and complex gene expression regulations such as splice leader trans-splicing and post-transcriptional editing (Lin, 2011; Lin et al., 2002; Zhang et al., 2007). Deep sequencing of dinoflagellates using RNA-seq methods have partly facilitated a means to address these challenges (Ryan et al., 2014; Shi et al., 2017; Stüken et al., 2011; Williams et al., 2017; Wisecaver and Hackett, 2010; Zhuang et al., 2015). While the nutritional ecology of multiple HABs from diverse classes (Harke and Gobler, 2013, 2015; Ji et al., 2018; Wurch et al., 2019) has been assessed through the lens of transcriptomics, few studies have assessed dinoflagellates (Lie et al., 2017, 2018; Luo et al., 2017; Morey et al., 2011; Rubin et al., 2019; Shi et al., 2017; Zhuang et al., 2015) and, thus far, none have considered the nutritional ecology of the obligate mixotroph, *Dinophysis*.

Here, we explore the nutritional ecology of *Dinophysis* using two approaches. First, ^{15}N tracer experiments were performed to quantify the concentration-dependent uptake rates and associated kinetics of both pre-starved and pre-fed *Dinophysis* cultures grown with various nitrogenous compounds (nitrate, ammonium, urea). In parallel, the transcriptomic responses of *Dinophysis* cultures grown with multiple combinations of prey and nutrients were assessed using Illumina HiSeq. Transcriptomes were specifically assessed for expression of genes associated with photosynthesis, the use of nutrients, and pathways associated with heterotrophy.

2. Materials and methods

2.1. Cultures and culture maintenance

The cryptophyte, *Teleaulax amphioxeia* (K-0434, Scandinavian Culture Collection of Algae and Protozoa), and the ciliate, *Mesodinium rubrum* (MBL-DK2009), were isolated in 2009 from Helsingør Harbor, Denmark, and cultures were generously provided by PJ Hansen (Nielsen et al., 2013). During May 2013, clonal isolates of *D. acuminata* were established from Meetinghouse Creek, NY (40°56.314′N, 72°37.119′W) using 12-well culture plates (Corning, Corning, NY, USA). *Dinophysis acuminata* from Meetinghouse Creek was determined to be 100% identical to both *D. acuminata* from Narragansett Bay, Rhode Island, USA (accession number EU130566) and Northport Bay, New York (Hattenrath-Lehmann et al., 2013) by sequencing the mitochondrial cytochrome c oxidase 1 (*cox1*) gene (Campbell et al., 2010; Raho et al., 2008).

M. rubrum was fed *T. amphioxeia* weekly at a ratio of ~10:1 (prey: predator) and following complete consumption of the cryptophyte were fed to *Dinophysis acuminata* isolates weekly at a ratio of ~10:1 (prey: predator). To mimic field populations, two viable *D. acuminata* isolates from Meetinghouse Creek were combined and maintained in 2 L Pyrex Erlenmeyer flasks. All cultures were maintained using sterile *f*/2 (-Si) medium (883μmol L^{-1} nitrate and 36μmol L^{-1} phosphate; Guillard and Ryther, 1962) made from autoclaved and 0.2 μm-filtered aged coastal Atlantic Ocean water (40.7969°N, 72.4606°W) adjusted to a salinity of 25 and kept at 18 °C in an incubator with a 14:10 h light:dark cycle, illuminated by a bank of fluorescent lights that provided a light intensity of ~70 μmol quanta $m^{-2} s^{-1}$ to cultures.

2.2. Uptake kinetics of nitrogenous nutrients by starved and fed *Dinophysis* cultures

^{15}N tracer experiments were conducted to quantify uptake rates of various nitrogenous compounds (ammonium, nitrate, and urea) over a range of concentrations (2 - 100 μM of N) by pre-starved and pre-fed *Dinophysis* cultures. Prior to the initiation of the experiments a two-phase preconditioning period was implemented as per Hattenrath-Lehmann and Gobler (2015). For both phases, *M. rubrum* was provided to *Dinophysis* at ~1:1 ratio to reflect prey densities in the field where *Dinophysis* spp. is typically food-limited (Kim et al., 2008; Riisgaard and Hansen, 2009). The first phase was a two-week grow-out period in which *D. acuminata* was grown in nutrient replete medium (*f*/2 -Si, made from autoclaved, 0.2μm-filtered, aged seawater) and fed *M. rubrum* at a ratio of ~1:1 three times (day 0, day 7 and day 11). At the end of phase one (day 14), the culture was sieved through a 10 μm mesh (to rid the culture of residual *M. rubrum*) and subsequently washed into fresh *f*/2 (-Si). These *D. acuminata* cells were used to inoculate flasks for phase two of the preconditioning period where cultures were either starved or fed for another two weeks. The starved *D. acuminata* culture was maintained in nutrient replete medium (*f*/2 –Si), whereas the fed culture was maintained in the same medium and fed *M. rubrum* at a ~1:1 ratio four times during the two week period (every three to four days). This two-phased preconditioning period was implemented to: 1) generate sufficient biomass for large experiments, 2) ensure that the cultures that were fed and starved in phase 2 originated from healthy, well fed cultures and 3) ensure that all cultures used for experiments were handled in the same fashion. Immediately prior to the start of the experiments, both starved (herein referred to as pre-starved) and fed (herein referred to as pre-fed) cultures were sieved using a 10 μm mesh filter and washed into freshly made *f*/2 (–N and –Si) to ensure both cultures had the same background nutrient concentrations, minimal bacterial densities and to remove any residual *M. rubrum*. Each culture was then distributed to sterile, triplicate 50 ml polystyrene flasks and controls were established (no tracer or nitrogen added). Triplicate flasks were amended with either nitrate, ammonium or urea at final concentrations of 2, 5, 10, 25, 50, and 100 μM of N; 90% was added as ^{14}N while the remaining 10% was ^{15}N labeled substrate. Flasks were incubated for 1 hour in an 18 °C incubator illuminated by a bank of fluorescent lights that provided a light intensity of ~70 μmol quanta $m^{-2} s^{-1}$. Turnover rates of nutrients were assumed to be minimal given the short incubation period (Glibert

et al., 1982). In addition, contributions of bacteria to the ^{15}N signal were considered minimal given that 1) cultures were sieved using a 10 μm mesh filter prior to the start of the experiments and 2) the use of glass fiber filters (GF/F) would retain only a small fraction of bacteria (Lee et al., 1995).

At the end of the incubation, treatments in addition to control samples (no tracer or nitrogen added) were filtered onto pre-combusted (4 h @ 450 °C) 25 mm GF/F glass fiber filters and frozen (−20 °C). Samples were then dried at 60 °C and pelleted for particulate nitrogen and ^{15}N analysis via continuous flow isotope ratio mass spectrometry (IRMS) by the UC Davis Stable Isotope Facility. Specific uptake rates were calculated according to the mixing model of Montoya et al. (1996) using equations from Orcutt et al. (2001) and converted to *Dinophysis* cell specific uptake rates. A Michaelis–Menten curve fitting function within Kaleidagraph (v 4.5, Synergy Software) was used to determine V_{max} (maximum cell specific uptake rates) and K_S (half saturation constant) and the nutrient affinity coefficient, α, was calculated from V_{max}/K_S. Differences in maximum cell specific uptake rates were elucidated using two-way ANOVAs where pre-conditioning (pre-starved or pre-fed) and nutrient source were the main effects using Sigma Stat software embedded within Sigma Plot 11.0. The Holm-Sidak method was used for post-hoc comparison tests with statistical significance set at an alpha of 0.05.

2.3. Dinophysis transcriptome experiments

An experiment was conducted to assess the effects of nutrients and prey on *Dinophysis* gene expression. Prior to the start of the experiment, *Dinophysis* was grown in nutrient replete medium (*f*/2 -Si, made from autoclaved, 0.2μm-filtered, aged seawater) and was fed *M. rubrum* at a ~1:1 ratio four times (every three to four days) during a two week grow-out period. Immediately prior to the start of the experiment, the culture was sieved using a 10 μm mesh filter and washed into freshly made *f*/2 (–N and –Si) to ensure there was no residual nitrogen or *M. rubrum* in the stock culture. The sieved stock culture was used to inoculate triplicate 500 ml Erlenmeyer flasks with 310 ml of *Dinophysis* culture (in freshly made *f*/2 –N and –Si) at an initial density of 1050 cells ml^{-1}. Triplicate flasks of five treatments were established as follows: 1) nitrate added in 12.5 μM daily doses for four days (total of 50 μM), 2) ammonium added in 12.5 μM daily doses for four days (total of 50 μM), 3) *M. rubrum* at an initial density of 1050 cells ml^{-1} (referred to as 'prey'), and 4) *M. rubrum* at an initial density of 1050 cells ml^{-1} with ammonium added in 12.5 μM daily doses for four days (total of 50 μM; referred to as 'ammonium + prey'), and 5) no nutrients or prey added (referred to as the control). Immediately prior to the start of the experiment, *M. rubrum* was transferred to *f*/2 (–N, -Si), allowed to vertically migrate to the top of the flask and surface aggregates were transferred to another flask with *f*/2 (–N, -Si). This was done multiple times to reduce nutrient carry over into experimental flasks. Nutrients were added to appropriate experimental flasks in doses to avoid potential toxic effects of high ammonium concentrations (Collos and Harrison, 2014) seen in previous nutrient amendment experiments (Hattenrath-Lehmann and Gobler, 2015). While nitrate does not elicit a toxic effect, it was added in the same fashion as ammonium to ensure experimental flasks were treated similarly. Flasks were incubated (as above) at 18 °C for a four-day period. Ambient nutrient concentrations in experimental flasks were measured daily (after the addition of nutrients for the first time point (day 0) and prior to the addition of nutrients for every time point thereafter). Filtrate was made using precombusted (4 hr @ 450°C) glass fiber filters (GF/F, 0.7 μm pore size) and frozen in acid washed scintillation vials. Filtrate was analyzed colorimetrically on a Lachat QuikChem 8500 flow injection analysis system (Lachat Instruments; Hach Company, Colorado, USA) with analyses proceeding only after 100% recovery of standard reference materials for nitrate and ammonium (SPEX©) were achieved. Every two days, a 5 mL aliquot from each flask was fixed in Lugol's iodine (final concentration= 2%) and cells were enumerated with a 1 mL Sedgewick-Rafter chamber using a compound microscope. After four days, *Dinophysis* cells were harvested from each experimental flask by removing 50 ml of well-mixed culture (51,000–154,000 cells per pellet), concentrating the aliquot on a 10 μm mesh filter, rinsing thoroughly and immediately backwashing cells into a 15 ml centrifuge tube using fresh *f*/2 (–N and –Si). *Dinophysis* cell pellets were made immediately by centrifuging at room temperature at 1700 rcf for 15 min and aspirating the supernatant without disturbing the cell pellet. Trizol® was immediately added to all cell pellets and kept frozen at −80 °C until RNA extraction.

To assess differences in cell densities between treatments (control, prey, ammonium, nitrate, ammonium + prey) two-way repeated measures ANOVAs (ANOVARs) were conducted using Sigma Plot v11.0. Each experimental flask was considered a subject and factors were treatments and time. The Holm-Sidak method was used for post-hoc comparison tests, with statistical significance set at an alpha of 0.05.

2.4. Transcriptome sample processing and sequencing

RNA was isolated and cDNA synthesized for all samples (triplicate flasks for each treatment at day four) using dinoflagellate spliced leader-based transcriptome profiling according to Zhang et al. (2007) and Zhuang et al. (2015). Because our cDNA libraries were prepared using DinoSL, which is specific to dinoflagellate nuclear mRNAs (Zhang et al., 2007), the expressed genes identified in this study and discussed here are genes from the *Dinophysis* nuclear genome. The modified random primer Illu-N9b was used to synthesize the first-strand cDNA, and 5′-end intact double stranded cDNA libraries were PCR amplified with Illu-D_SLb-Read1 (Table S1). The PCR conditions were 1 cycle of 95 °C for 3 min, 5 cycles of 95 °C for 15S, 56 °C for 30S, and 72 °C for 30S, followed by 25 cycles of 95 °C for 15S, 68 °C for 60S, and 1 cycle of 72 °C for 5 min. For each cDNA sample, 10 PCR reactions were run and combined, and the PCR products purified according to Zhang et al. (2007). For each sample, equal amounts of the triplicate samples were mixed, and size fractionated via gel electrophoresis in an agarose gel to cut the cDNAs into two size fractions (Dino-S, 350–500 bp and Dino-L: 500–900 bp). DNA samples were purified from the agarose gel using Zymoclean™ Gel DNA Recovery kit (Zymo Research). For both Dino-S and Dino-L fractions, unique indices were added to the following 5 cDNA libraries: 1) Control-T4, 2) Prey-T4, 3) Ammonium-T4, 4) Ammonium+prey-T4, and 5) Nitrate-T4 using Nextera XT DNA Sample Preparation Index Kit using the method of preparing amplicons for the Illumina MiSeq System with modification (Table S2; Illumina). PCR was run using the following conditions: 1 cycle of 95 °C for 3 min, 10 cycles of 95 °C for 15S, 55 °C for 30S, and 72 °C for 30S, and 1 cycle of 72 °C for 5 min. Only the Dino-S size fraction was processed further and used for sequencing. The cDNA libraries with the indices were purified with Pronex Size Selective Purification System (Promega) following the manufacturers protocol to enrich fragments of ~550 bp. The concentration of each library was quantified using the NEBNext® Library Quant Kit (New England Biolabs) and pooled based on DNA concentration for a final concentration of 3.2 nM. Paired end sequencing was conducted using 2 lanes of Illumina HiSeq2500 Rapid Run.

2.5. Transcriptome analysis

Quality trimming was conducted on raw reads to remove adapter sequences and poor quality data with TrimmomaticPE (version 0.36; Bolger et al., 2014). The parameters were set as follows: ILLUMINACLIP: adaptor_nextera.fasta:2:30:10 LEADING:5 TRAILING:5 SLIDINGWINDOW: 4:15 MINLEN:50, with a custom made Nextera adapter file. Using Kraken (version 0.10.6; Wood and Salzberg, 2014), rRNA and general plasmid like sequences were removed using the SILVA database of SSU and LSU sequences (release 128; Quast et al., 2012) and NCBI database of plasmid sequences. The resulting clean reads were evaluated with FastQC (v0.11.5; Andrews, 2010) and used for further analyses.

Trimmomatic unpaired reads were merged to the end of the respective reads files of the paired fragments for assembly. All the clean reads from different treatments and lanes were first pooled and normalized using Trinity's (version v2.8.4; Grabherr et al., 2011) in-silico normalization module, then denovo assembled into transcripts using Trinity's paired-end mode with default settings. The candidate open reading frames (ORFs) and deduced amino acid sequences were obtained using TransDecoder (version 5.5.0, https://transdecoder.github.io/; Haas et al., 2013) utilizing the Blastp (BLAST+ version 2.9.0; Camacho et al., 2009) and Hmmscan (HMMER version 3.2.1; Eddy, 2009) results. Diamond blastx (evalue=$1e^{-3}$) was used to annotate transcripts against Phylodb, (a database comprised of peptides obtained from KEGG, GenBank, JGI, Ensembl, CAMERA, and various other repositories (available for download at https://scripps.ucsd.edu/labs/aallen/data/) and NCBI NR databases. Homology annotation was also conducted using BLAST (with evalue $1e^{-3}$ as cutoff) to search against the UniProt_Swiss-Prot database (release 2016.08). InterProScan (version 5.39–77.0; Jones et al., 2014) was used to obtain GO and InterPro annotations based on Transdecoder identified peptide sequences. Blast and hmmscan results were systematically combined using Trinotate (version 3.0.1; Bryant et al., 2017). GO annotations were integrated from UniPort and InterProScan annotations. KEGG annotations were obtained from the

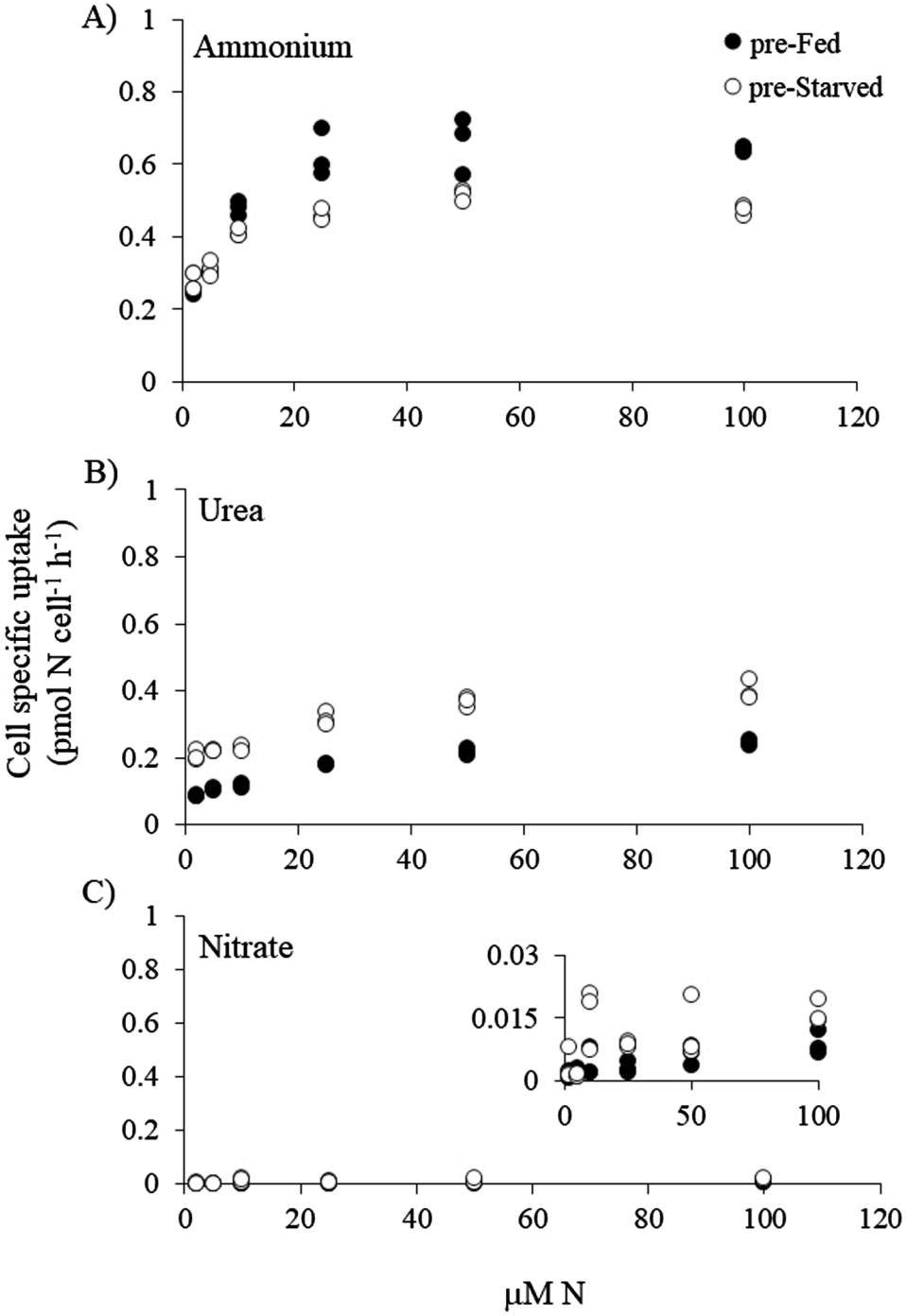

Fig. 1. ^{15}N tracer experiment: Cell specific N uptake rates (pmol N $cell^{-1}$ h^{-1}) of pre-starved (white circles) and pre-fed (black circles) *Dinophysis acuminata* cultures at varying concentrations (2 - 100 µM of N) of A) ammonium, B) urea, and C) nitrate. 90% of N was added as ^{14}N while the remaining 10% was ^{15}N labeled substrate. Inset is the nitrate figure expanded.

combination of the annotation using GhostKOALA service from KEGG (Kanehisa et al., 2016) and UniProt derived KO annotations.

Read counts of transcripts were obtained with Kallisto (version 0.46.0; Bray et al., 2016) by mapping the clean reads of each sample to the assembled transcriptome (Supplementary dataset 1). Differential gene expression was performed using the R package Sleuth3 (version 0.28–1; Pimentel et al., 2017) based on read counts, in which only transcripts with read counts of at least 5 in half of the samples were used in the analysis to ensure data quality. To obtain KEGG gene level expression, the transcript expression was aggregated utilizing the gene aggregation option within Sleuth. Sleuth generates b value (beta value, Wald only), a biased estimator of the fold change compared to ambient control (no nutrients, no prey) and also gives the statistical significance (q-value). KEGG genes with fold change ≥4 and adjusted p-value ≤0.05 between two conditions were considered to be significantly differentially expressed. To identify the cellular responses linked with each treatment, KO genes that were uniquely expressed in each treatment and those that were shared between the ammonium and ammonium + prey, and prey and ammonium + prey were identified. Following the KEGG database classification at level B, the identified KO genes were classified into functional pathways (Table S4 and Table S5). KO genes that belonged to amino acid metabolism, carbohydrate metabolism, energy metabolism (including nitrogen metabolism), folding, sorting and degradation (protein related), lipid metabolism and transport, and catabolism (including phagosomes, lysosomes, endocytosis), along with the enzymes in BRITE category were identified. The remaining pathways were included as other cellular pathways. The raw read files (see Supplementary dataset 2 for SRA accessions), assembled transcriptomes, and gene expression data are available for download through NCBI BioProject: PRJNA632555. The Transcriptome Shotgun Assembly project has been deposited at DDBJ/EMBL/GenBank under the accession GIOG00000000. The version described in this paper is the first version, GIOG01000000.

3. Results

3.1. N uptake kinetics of pre-starved and pre-fed Dinophysis cultures

N uptake kinetics for pre-starved *Dinophysis* cultures displayed Michaelis-Menten type behavior for all substrates (ammonium, urea and nitrate) tested, with nitrate having the lowest correlation coefficient (R^2 for nitrate= 0.61, ammonium= 0.93, and urea= 0.85; Fig. 1, Table 1). Maximum cell-specific uptake rates for pre-starved *Dinophysis* cultures were significantly higher for ammonium (0.5 ± 0.01 pmol N cell^{-1} h^{-1}) than other compounds, followed by urea (0.37 ± 0.02 pmol N cell^{-1} h^{-1}) with nitrate being 25-fold lower (0.02 ± 0.003 pmol N cell^{-1} h^{-1}; $p<0.001$ for all, two-way ANOVA; Fig. 1, Table 1). Half saturation constants (K_s) were 2.0 ± 0.3, 3.0 ± 0.7 and 7.8 ± 6.1 μM N for pre-starved *Dinophysis* cultures provided ammonium, urea and nitrate, respectively, while affinity coefficients were 0.25, 0.12 and 0.002 (Table 1).

N uptake kinetics for pre-fed *Dinophysis* cultures followed a similar pattern to those of pre-starved *Dinophysis* cultures (R^2 for nitrate= 0.73, ammonium= 0.96, and urea= 0.94; Fig. 1, Table 1). Maximum cell specific uptake rates for pre-fed *Dinophysis* cultures were significantly higher for ammonium (0.70 ± 0.02 pmol N cell^{-1} h^{-1}), followed by urea (0.25 ± 0.01 pmol N cell^{-1} h^{-1}) with nitrate being more than 70-fold lower (0.01±0.003 pmol N cell^{-1} h^{-1}; $p<0.001$ for all, two-way ANOVA; Fig. 1, Table 1). Half saturation constants (K_s) were 4.7 ± 0.71, 7.2 ± 1.3 and 39±29 μM N, while affinity coefficients were 0.15, 0.03 and 0.0003, for pre-fed *Dinophysis* cultures provided with ammonium, urea and nitrate, respectively (Table 1). Nutrient source significantly ($p<0.001$) affected *D. acuminata* maximum uptake rates, but preconditioning (pre-starved vs. pre-fed) did not. However, there was a significant interaction between these factors as the response to preconditioning was dependent on nutrient source ($p<0.001$, two-way ANOVA, Table 1) as there was synergy between the ammonium grown culture and feeding: ammonium-grown cultures that were pre-fed had higher uptake rates than pre-starved cultures, whereas for urea and nitrate, pre-starved cultures grown with the nutrients outgrew pre-fed cultures grown with nutrients. Maximum uptake rates of all treatments were significantly different from each other with the exception of pre-starved vs pre-fed cultures offered nitrate ($p<0.001$, two-way ANOVA, Table 1).

3.2. Growth of Dinophysis under varying nutritional conditions for transcriptomic analyses

Both nutrient treatment and time significantly affected *D. acuminata* densities during the transcriptome experiment and there was a significant interaction between these factors as the response to nutrients changed over time ($p<0.001$ for all, two-way ANOVAR; Fig. 2). Densities of *D. acuminata* grown on nitrate did not change significantly over the course of the experiment, while cells in the control increased slightly but significantly from $t = 0$ to $t = 2$ ($p<0.05$, two-way ANOVAR; Fig. 2) but then decreased again ($t = 4$). *D. acuminata* densities in prey, ammonium and ammonium + prey treatments increased significantly ($p<0.001$ for all, two-way ANOVAR) over time, resulting in a 110%, 90% and 170% increase in cell densities, respectively, from the start ($t = 0$) to the end ($t = 4$) of the experiment (Fig. 2). During $t = 2$, the only significant ($p<0.05$, two-way ANOVAR) differences among treatments were between prey-, ammonium-, and ammonium + prey- treatments vs. the nitrate amendment with the former having higher cell densities (Fig. 2). During $t = 4$, however, all experimental treatments were highly and significantly ($p<0.001$ for all, two-way ANOVAR) different from each other with the exception of the nitrate vs control, and the ammonium vs prey treatments (Fig. 2). For $t = 4$, ammonium + prey (2829±226 cells L^{-1}) had the highest *Dinophysis* densities of any treatment followed by prey (2160±126 cells L^{-1}) and ammonium (1997±156 cells L^{-1}) treatments with the addition of ammonium + prey having an additive effect on cell densities.

Ammonium concentrations in ammonium addition treatments were drawn down to levels that were lower than the amount added, while levels of ammonium in the nitrate, control and prey treatments were drawn down to <2 μM on $t = 1$ and remained at this level throughout the experiment (Fig. 2). Nitrate concentrations in the nitrate treatment increased steadily and were similar to the amount added, while the concentration of nitrate in all other treatments remained <1 μM over the

Table 1
Maximum cell specific uptake rates (V_{max}; pmol N cell^{-1} h^{-1}), half saturation constant (K_s; μM N), affinity coefficient (α; V_{max}/K_S) and R^2 of Michaelis-Menten parameters for pre-starved and pre-fed *Dinophysis* cultures using ammonium, urea and nitrate as substrate. Mean ± SD. Letters indicate Holm-Sidak multiple comparison results ($p<0.001$).

	Ammonium		**Urea**		**Nitrate**	
	Pre-Fed	Pre-Starved	Pre-Fed	Pre-Starved	Pre-Fed	Pre-Starved
V_{max}	0.70±0.02^{a}	0.5 ± 0.01^{b}	0.25 ± 0.01^{c}	0.37± 0.02^{d}	0.01±0.003^{e}	0.02±0.003^{e}
K_s	4.7 ± 0.71	2.0 ± 0.3	7.2 ± 1.3	3.0 ± 0.7	39±29	7.8 ± 6.1
R^2	0.96	0.93	0.94	0.85	0.73	0.61
α	0.15	0.25	0.03	0.12	0.0003	0.002

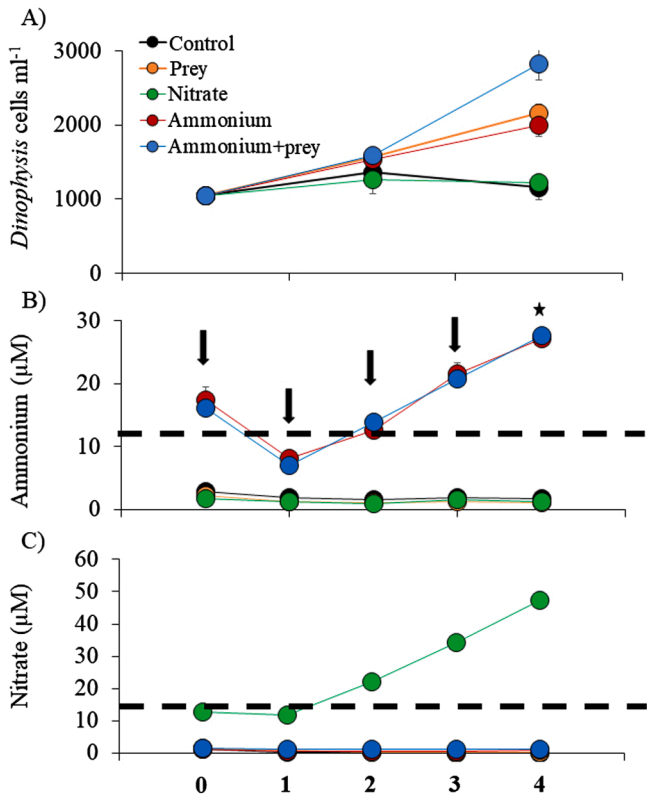

Fig. 2. Transcriptome experiment: A) Growth of *Dinophysis acuminata* (cells mL^{-1}) cultures provided varying nitrogenous nutrients. B) Ammonium and C) nitrate concentrations (µM) were measured after addition of nutrients only at $t = 0$. Black arrows indicate time points in which nutrients were added and stars represent time points in which cells were harvested for RNA extraction. Measurements for all other days represent nutrient measurements made before the daily nutrient additions. Black hatched lines represent the concentration at which nutrients were added daily. (For interpretation of the references to colour in this figure legend, the reader is referred to the web version of this article.)

course of the experiment (Fig. 2).

3.3. Transcriptomic responses of Dinophysis under varying nutritional conditions

Most of the variability (PC1=86.2%) in expression patterns of transcripts following supplementation with different nutrients and/or prey indicated that transcript abundances separated the control and nitrate treatments from the ammonium, prey, and ammonium + prey (Fig S1). A smaller percentage (PC2=10%) of the changes in transcript abundances separated the ammonium, prey, and ammonium + prey treatments (Fig S1). Similarly, hierarchical clustering revealed that the control and nitrate treatments, and ammonium and ammonium + prey treatments grouped close to each other while the prey only treatment clustered closest to but separately from the ammonium and ammonium + prey treatments (Fig S2). These changes in gene expression were further assessed through evaluation of aggregated KEGG KO gene expression.

Transcripts encoding a total of 2082 unique KO genes with KEGG database IDs (KO IDs) belonging to 319 KEGG pathways were identified, of which 1857, 1882, 1843, and 1885 KO genes in nitrate, ammonium, prey and ammonium + prey, respectively were filtered (Sleuth with default parameters) and considered for differential gene expression. Of these, 291, 269, 263 and 305 KO genes were differentially expressed in nitrate, ammonium, prey and ammonium + prey, respectively, compared to the control (Fig. 3, corrected p-value <0.05 genes > 4-fold

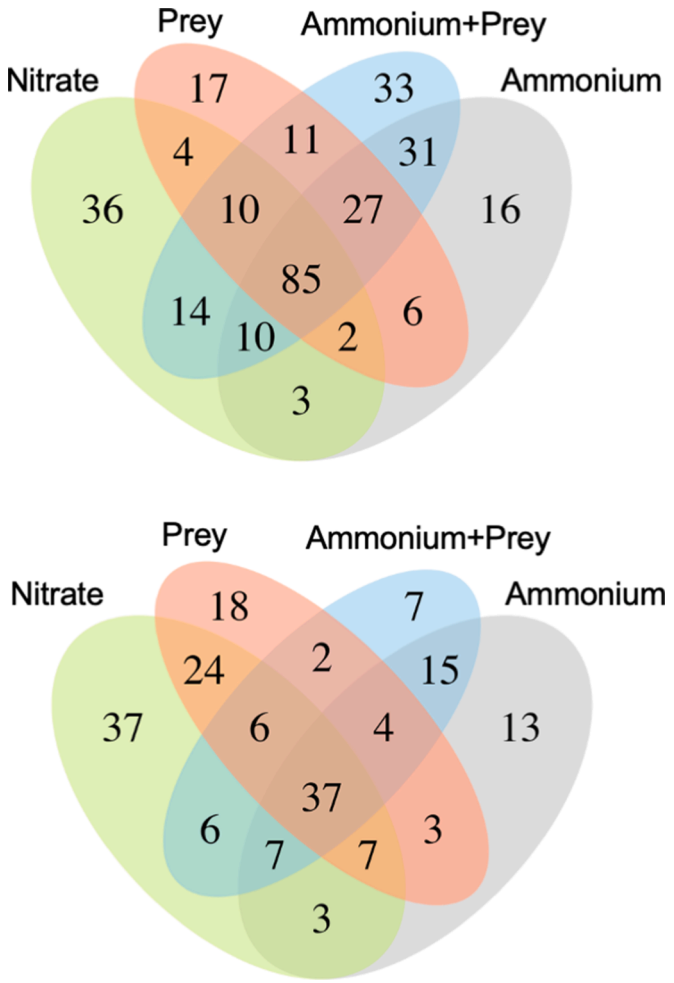

Fig. 3. Transcriptome experiment: The number of significantly differentially expressed KEGG KO genes (adjusted p-value <0.05 and 4 fold change) in the four treatments and combination of treatments in comparison to starved control condition. a) KO genes that had an increase in transcript abundance and b) KO genes that had a decrease in transcript abundance. Colors correspond to treatments: green (nitrate), coral (prey), blue (ammonium + prey), and gray (ammonium). (For interpretation of the references to colour in this figure legend, the reader is referred to the web version of this article.)

TPM change were considered expressed). Among the differentially expressed genes, the ammonium + prey treatment had the most KO genes (221) with significantly higher transcript abundances, while the nitrate treatment had the highest number of genes with a decrease in transcript abundances (127, Fig. 3). Further, 85 genes with increased transcript abundances and 37 genes with decreased transcript abundances were common among the four treatments (Table S3 & Fig 3). Between the treatments, ammonium and ammonium + prey had the most common KO genes (31) with increases in transcript abundances while the nitrate and the prey treatments had the most common genes (24) with decreases in transcript abundances (Table S3, Fig 3). Individually, the nitrate treatment had the highest number of genes with increased- and decreased- transcript abundances (36 and 37 KO genes) that were unique to the treatment, followed by the ammonium + prey treatment (33 KO genes with uniquely increased transcript abundances), the prey treatment (18 and 17 unique KO genes with decreased- and increased- transcript abundances), and the ammonium treatment (16 and 13 KO genes with increased- and decreased- transcript abundances), and the ammonium + prey treatment (7 with decreased abundances). To avoid redundancy, we describe and interpret the responses of different genes from different treatments in each of the KEGG categories in the

Discussion.

4. Discussion

4.1. N uptake kinetics of pre-starved and pre-fed Dinophysis cultures

Despite being a kleptoplastidic mixotroph, *Dinophysis*, like most phytoplankton, displayed Michaelis-Menten type kinetics for nitrogenous nutrients (Bonachela et al., 2011) as well as differences between pre-fed and pre-starved cultures. Pre-fed cultures offered ammonium had a significantly higher V_{max} than pre-starved cultures, while pre-starved cells had a higher affinity coefficient and lower K_s. In contrast to the ammonium-grown cultures, pre-starved cultures provided with urea and nitrate had a higher V_{max} and affinity coefficient, and lower K_s compared to pre-fed cultures (Fig. 1, Table 1). Consistent with previous ^{15}N uptake experiments (Hattenrath-Lehmann and Gobler, 2015), both pre-starved and pre-fed cultures assimilated nitrate but at very low rates (<0.02 pmol N cell^{-1} h^{-1}; 50 – 70-times lower than ammonium) and pre-starved cells had higher uptake rates than pre-fed cells. Cultures grown with ammonium had a high V_{max} and affinity coefficients, and low K_s for both pre-starved and pre-fed cultures collectively demonstrating *Dinophysis'* preference for this N source. These findings are similar to an ecosystem-based *Dinophysis* experiment by Seeyave et al. (2009) that demonstrated ammonium uptake was highest followed by urea and nitrate. Half saturation constants (Ks) for ammonium, urea and nitrate were within range of those typically reported for dinoflagellates, including mixotrophic species (Kudela et al., 2010a, 2008; Smayda, 1997). To our knowledge this is the only report of concentration-dependent N uptake rates by a kleptoplastidic dinoflagellate.

4.2. Transcriptomic and physiological responses of Dinophysis under varying nutritional conditions

Dinophysis is a kleptoplastidic dinoflagellate, and consistent with this, the observed nutritional response was indicative of a dependency on both autotrophic and heterotrophic biochemistry. Transcriptomic analyses conducted by Wisecaver and Hackett (2010) found that *Dinophysis acuminata* has far fewer nuclear-encoded plastid genes than most fully photosynthetic dinoflagellates. Moreover, *Dinophysis* has limited functional control over these plastids and is unable to maintain them over time (Wisecaver and Hackett, 2010). This, in addition to increased cell yields when offered both ammonium + prey (*Mesodinium*) and the synergistically higher ammonium uptake rates when pre-fed provides further evidence that *Dinophysis* is a mixotroph that relies on exogenous ammonium.

4.3. Growth on nitrate

In the nitrate treatment, glutamine synthetase (K01915 [EC:6.3.1.2], Fig 4 and 5, Table S5), which catalyzes the condensation of glutamate and ammonium to glutamine, uniquely had significantly lower transcript abundances indicating a decrease in ammonia assimilation through the GO-GAT pathway. In addition, there was a significant decrease in carbonic anhydrase (K18246, [EC:4.2.1.1], Table S6) transcript abundance indicating a down-regulation of the inorganic carbon incorporation into biological pathways. Although nitrate was supplied, an increase in transcript abundances of nitrate and nitrite reductases was not observed, nor was any nitrate drawdown observed during the transcriptome experiment. Furthermore, nitrate uptake during ^{15}N experiments was minimal. In the transcriptome, one transcript for each nitrate reductase (TRINITY_DN13393_c0_g1_i1, Table S7) and nitrite reductase (TRINITY_DN12577_c0_g1_i1, Table S7) were annotated by the UniPort database, whereas four other transcripts were annotated for nitrate/nitrite transporter (Table S7) using UniProt and UniRef90 databases. Of these, one transcript showed a non-significant increased abundance, another showed no significant change and, reads related to transcripts annotated as nitrite reductase and two of nitrate/nitrite transporter were not present in the nitrate treatment. Thus, it appears that *D. acuminata* does not actively acquire nitrate and convert to ammonium. These observations of nuclear transcripts are consistent with the finding that nitrate reduction reactions take place within the plastid of some dinoflagellates (Fritz et al., 1996) and that *Dinophysis* has limited functional control over its kleptoplastids (Wisecaver and Hackett, 2010). Garcia-Portela et al. (2020) evaluated 33 dinoflagellate reference transcriptomes and found that *Dinophysis* had the lowest number of nitrate transporter and nitrate reductase homologs. Despite the inability of *D. acuminata* to use nitrate, it may still acquire N indirectly from nitrate, perhaps from a non-specific ion transporter or via bacterial reduction of nitrate to ammonium at the cell surface. This may, in part, explain the minute rates of nitrate uptake seen during ^{15}N experiments here and in other studies (Hattenrath-Lehmann and Gobler 2015; García-Portela et al., 2020). Further, allantoinase (K01466 [EC:3.5.2.5], Fig 4 and 5, Table S4), a hydrolase that is involved in the degradation of purine derivative allantoin had uniquely high transcript abundances in the nitrate treatment, indicating that the N limited cells were acquiring N from nitrogen-rich organic compounds like purines and its derivatives (Werner and Witte, 2011).

Beyond N metabolism genes and the lack of *Dinophysis* growth when offered nitrate (Hattenrath-Lehmann and Gobler, 2015; Hattenrath--Lehmann et al., 2015; Tong et al., 2015), the effects of N limitation were also evident in the other metabolic processes. The nitrate treatment had the highest number of genes with decreased transcript abundances (127 KO genes, Fig. 3), overall indicating a lower metabolic activity. Pyruvate metabolism forms the link between the citrate cycle and glycolysis, which, in turn, are the central metabolic pathways that link many other pathways. Pyruvate metabolism enzymes, pyruvate carboxylase (K01958 [EC:6.4.1.1]) and D-lactate dehydrogenase (cytochrome) ([EC:1.1.2.4], K00102, Fig 4, Table S5) had uniquely lower transcript abundances in the nitrate treatment indicating a reduced metabolic activity (Jitrapakdee et al., 2008). In addition, photosystem (PS) II P680 reaction center D1 protein (K02703, [EC:1.10.3.9], Fig 4 and 5, Table S5) had uniquely lower transcript abundances indicating a reduction in photosynthesis. However, there was no corresponding decrease in PS I or plastocyanin (PC). On the contrary, PS I and PC related genes increased transcript abundances (K02689, K2638, Fig 5, Table S6) indicating a differential regulation of the PS I, PS II and photosynthetic electron transport chain. Such differential regulation has been reported in a previous study (Berges et al., 1996) and suggests that N limitation primarily effects PS II, particularly the depletion of PS II D1 protein. In our analysis, photosystem II CP43 chlorophyll apoprotein (K02705) also displayed a decreased abundance, though not uniquely. Fructose bisphosphatase (EC 3.1. 3.11, K03841; involved in gluconeogenesis and the Calvin cycle, Fig 4 and 5, Table S5) showed uniquely lower transcript abundances indicating a corresponding decrease in carbohydrate synthesis alongside the reduced CO_2 assimilation and photosynthesis. While the oxidative phosphorylation pathway was stymied via decreased transcript abundances of 6-phosphogluconolactonase ([EC:3.1.1.31] K01507, Fig 4 and 5, Table S5), enhancement of non-oxidative phosphorylation was observed via increased transcript abundances of D-xylose reductase ([EC:1.1.1.307], K17743, Fig 4 and 5) indicating potential utilization of alternative sources of energy (Neuhauser et al., 1997). Fatty acid biosynthesis and degradation can be closely linked with N availability (Chen and Johns, 1991; Ikaran, 2015). Long-chain-fatty-acid-CoA ligase ACSBG (K15013 [EC:6.2.1.3], Fig 4 and 5, Table S4) had uniquely higher transcript abundances in the nitrate treatment. This enzyme is involved in both the fatty acid biosynthesis and fatty acid degradation but the increased abundance of transcripts for the malate synthase [EC:2.3.3.9] (Fig 5, Table S6) suggested an activation of the glyoxylate cycle in which acetate from degraded fatty acids are used for biosynthesis of carbohydrates. Additionally, 2−isopropylmalate synthase [EC:2.3.3.13], involved in leucine

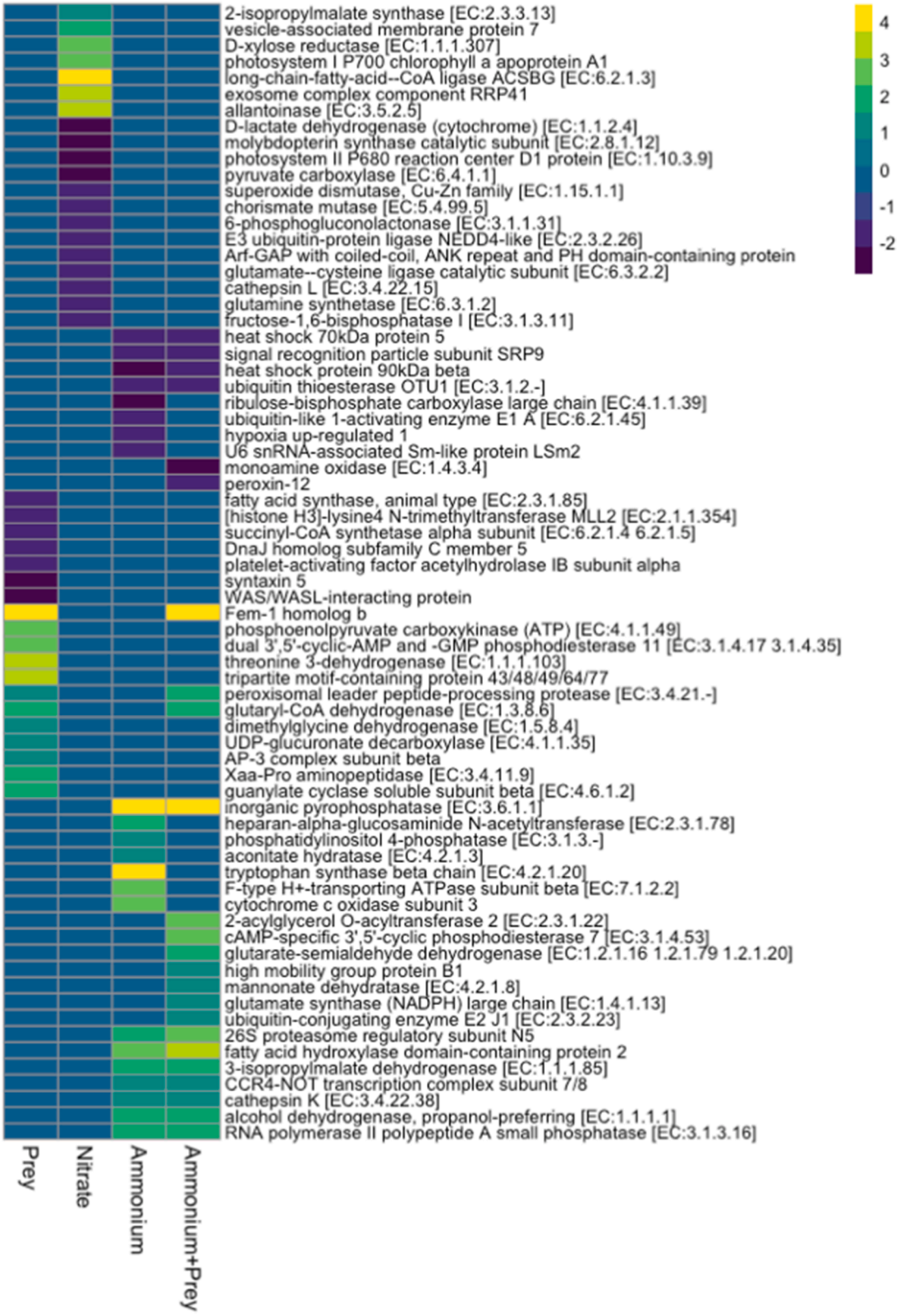

Fig. 4. Transcriptome experiment: Gene expression levels of KEGG KO genes that were differentially expressed (adjusted pvalue <0.05 and 4 fold change) uniquely in either of the treatment or shared between ammonium and ammonium+prey treatment or prey and ammonium+prey treatment. Other differentially regulated genes that are discussed in the manuscript can be accessed in the supplementary tables S4-S6. Treatments are clustered by calculating the distance using the correlation method and observations were not scaled. Colors correspond to the expression levels in terms of b-value (log fold TPM as calculated by Sleuth) represented in the legend scale. The plot was generated in R using the pheatmap package. (For interpretation of the references to colour in this figure legend, the reader is referred to the web version of this article.)

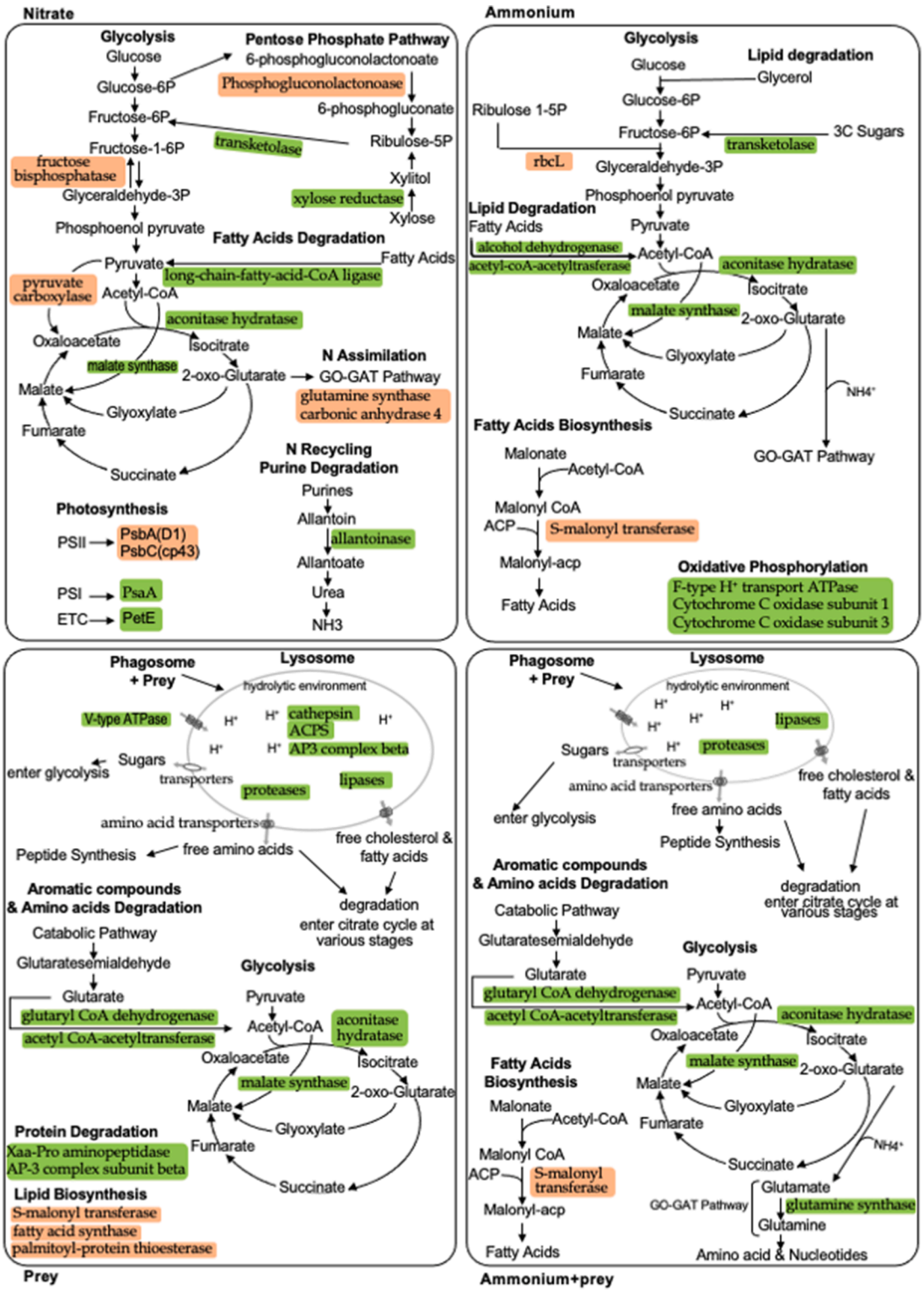

Fig. 5. Transcriptome experiment: Summary of the observed changes in the metabolic pathways as a response to nitrate, ammonium, prey and ammonium-prey treatments. KEGG KO genes that showed an increase (green) and decrease (orange) in abundance are shown. (For interpretation of the references to colour in this figure legend, the reader is referred to the web version of this article.)

biosynthesis, vesicle−associated membrane protein 7, involved in vesicle trafficking, and exosome complex component RRP41, involved in cellular RNA processing and degradation, all showed increased abundance thus helping to maintain cellular metabolism under stress. Collectively, these findings indicate that although genes associated with nitrate were found in the transcriptome of *D. acuminata, D. acuminata* does not actively acquire and assimilate nitrate into biological pathways. In fact, exposure to nitrate seems to elicit a cascading response typical of nitrogen starvation that was more evident compared to its starved control. This may indicate that the presence of low nitrate levels may initiate a type of cell dormancy in *D. acuminata*, a strategy many microalgae utilize to overcome stress conditions (Bravo and Figueroa,

2014).

4.4. Growth on ammonium

In contrast to nitrate, ammonium clearly stimulated multiple metabolic pathways in *Dinophysis*. In the treatment where *Dinophysis* was offered only ammonium, there were no significant changes in the KEGG KO genes related to N metabolism and several isoforms of ammonium transporters had significantly lower transcript abundances (4 of 18 isoforms, none increased in abundance, Table S7) indicating the cells might have accumulated sufficient N compounds (Frischkorn et al., 2014; Wurch et al., 2019, 2011) as evidenced by the drawdown in ammonium during the experiment. Alternatively, the ammonium transporters with decreased transcript abundances may have been high affinity ammonium transporters which were not needed given the higher levels of ammonium added (12.5 μM per day; Harke and Gobler, 2015). Beyond N metabolism, we observed a unique decrease in transcript abundances of the ribulose-bisphosphate carboxylase large chain (rbcL, K01601 [EC:4.1.1.39], Fig 4 and 5, Table S5) indicating reduced CO_2 acquisition and photosynthesis (energy metabolism), although other photosystem genes were unchanged. On the other hand, oxidative phosphorylation-related genes displayed higher transcript abundances, specifically F-type *H*+-transporting ATPase subunit beta (ATPeF1B, K02133, [EC:7.1.2.2]), inorganic pyrophosphatase (K01507, [EC:3.6.1.1]) (Fig 4, Table S4) and cytochrome c oxidase subunit 3 (COX3, K02262, 5, Table S6), indicating efficient generation of ATP likely through catabolic processes that were reflected in increased *Dinophysis* growth compared to control cultures. Carbohydrate metabolism genes uniquely or shared with the ammonium + prey treatment at higher transcript abundance included alcohol dehydrogenase (K13953 [EC:1.1.1.1]), 3-isopropylmalate dehydrogenase ([EC:1.1.1.85] K00052), phosphatidylinositol 4-phosphatase ([EC:3.1.3.-] K21797), and aconitate hydratase (K01681, [EC:4.2.1.3], citrate cycle; Fig. 4 and Table S4). In particular, the pyruvate metabolism-related genes in the ammonium treatment were also higher including malate synthase [EC:2.3.3.9], acetyl-CoA C-acetyltransferase [EC:2.3.1.9] and acetate kinase [EC:2.7.2.1], which evidences degradation of fatty acids (Table S6). In fact, transcript abundance for the fatty acid synthesis gene, [acyl-carrier-protein] S-malonyltransferase [EC:2.3.1.39] decreased while the fatty acid degradation genes, acetyl-CoA C-acetyltransferase [EC:2.3.1.9], alcohol dehydrogenase [EC:1.1.1.1] and 17-beta-estradiol 17-dehydrogenase / very-long-chain 3-oxoacyl-CoA reductase [EC:1.1.1.62 1.1.1.330] all increased in transcript abundance similar to the nitrate treatment (Fig 5 and Table S6). Thus, when *D. acuminata* was supplied with ammonium without the prey, later stage cell growth slowed leading to a shift in cellular metabolism towards catabolic processes for the cell survival. This may, in part, explain why *Dinophysis* densities were not significantly different among ammonium, and ammonium + prey treatments during $t = 2$, but by $t = 4$ cell densities in the ammonium + prey treatment were significantly higher than those in the ammonium treatment. We hypothesize the decrease in photosynthesis and growth and increase in fatty acid degradation might be due to lack of critical nutritional factors and co-factors that are derived from prey, further evidencing the importance of mixotrophy for *D. acuminata*.

4.5. Growth with prey only

In the prey only treatment (*M. rubrum* with no nutrients added), there were limited changes in gene expression involving N metabolism except for decreased transcript abundances of carbonic anhydrase 4 (K018246, [EC:4.2.1.1], Table S6) indicating a reduced CO_2 uptake and a possible reduced assimilation of ammonia into biological molecules related to a lack of available N as the ammonium + prey treatment which did not show this pattern. This provides evidence at the pathway level of the means by which growth on prey without ammonium may lead to slower growth compared to ammonium + prey, specifically the need for *Dinophysis* to couple its photosynthetic acquisition of C with the assimilation of exogenous N. Similar to the ammonium + prey treatment, transcripts encoding acetyl-CoA C-acetyltransferase and glutaryl-CoA dehydrogenase (Fig 5, Table S6) were at significantly higher abundances than the control evidencing increase in fatty acid degradation and conversion of glutarate degradation to acetyl-CoA. Significantly lower transcript abundances of [acyl-carrier-protein] S-malonyltransferase (K00645, [EC:2.3.1.39]), fatty acid synthase (K00665 [EC:2.3.1.85]) and palmitoyl-protein thioesterase (K01074 [EC:3.1.2.22], Fig 5, Table S6) suggest the down-regulation of the fatty acid biosynthesis pathway (Li-Beisson et al., 2013) collectively suggesting a shift away from biosynthesis and towards fatty acid degradation. However, of the 11 KO genes linked with fatty acid degradation, acetyl-CoA C-acetyltransferase (K00626, [EC:2.3.1.9], Fig 5, Table S6) and glutaryl-CoA dehydrogenase (K00252, [EC:1.3.8.6], Fig 4 and 5, Table S4), had significantly increased transcript abundances and none significantly decreased. Xaa-Pro-aminopeptidase (K01262, [EC:3.4.11.9]) and lysosomal gene AP-3 complex subunit beta (K12319, Fig 4 and 5, Table S4) had uniquely higher transcript abundances in the prey treatment indicating an up-regulation of protein degradation and perhaps a greater effort at extracting N from prey when ammonium was not available. With respect to phagosomes, V-type *H*+-transporting ATPase subunit E (K02150, Fig 5, Table S6) had increased transcript abundances indicating the need for maintaining the hydrolytically competent acidic environment within the phagosomes (Kissing et al., 2015). We hypothesize that the active maintenance of an acidic environment in the phagolysosome promotes the digestion of ingested prey (Kissing et al., 2015). Regarding carbohydrate metabolism, similar to the nitrate and ammonium treatment, malate synthase ([EC:2.3.3.9], Fig 5, Table S6) displayed a significant increase in transcript abundances indicating an active glyoxylate cycle and, potentially, fatty acid degradation. However, in the presence of prey this may be related to prey digestion rather than degradation of stored lipids. The increased abundance of phosphoenolpyruvate carboxykinase (ATP) [EC:4.1.1.49] a critical enzyme in gluconeogenesis from non-carbohydrate sources also evidences prey digestion. Other genes with a significant increase in transcript abundance included Fem-1b homolog, dual 3′, 5′−cyclic−AMP and −GMP phosphodiesterase 11 [EC:3.1.4.17 3.1.4.35], threonine 3−dehydrogenase [EC:1.1.1.103], tripartite motif−containing protein 43/48/49/64/77 and peroxisomal leader peptide−processing protease [EC:3.4.21.−] (Fig 4, Table S4 and S5), at times also in the ammonium + prey treatment. These genes again are likely involved in degrading and deriving nutrition from prey. Overall, the differential gene expression in response to the prey treatment involved genes related to prey digestion and deriving energy from the prey.

4.6. Growth on ammonium with prey

Among the four nutritional conditions assessed, the *Dinophysis* culture supplemented with ammonium + prey had the highest number of KEGG genes, with increased transcript abundances and lowest number of decreased transcript abundances indicating a state of high metabolic activity in the cells compared to the unamended control. Consistent with this, *Dinophysis* densities in this same treatment were significantly higher than all other treatments, and in ^{15}N uptake experiments *Dinophysis* pre-fed and provided ammonium had the highest uptake rates of any substrate tested. Significant increases in *Dinophysis* densities with the addition of ammonium + prey compared to cultures either fed *Mesodinium* (prey only) or grown with ammonium only was also observed by Hattenrath-Lehmann and Gobler (2015). Paralleling the drawdown of ammonium observed in this treatment, KEGG genes revealed an increase in ammonium utilization through the activation of the enzyme glutamate synthase (K00265 [EC:1.4.1.13], Fig 4 and 5, Table S4). In comparison, this gene was unaffected in the ammonium

only treatment indicating a greater rate of amino acid synthesis in this combined treatment. However, the ammonium transporter genes were unaltered or displayed decreasing transcript abundances at the isoform-level (4 of 16 isoforms, Table S7) similar to the ammonium only treatment. Given some high affinity ammonium transporters are induced as a symptom of N limitation in eukaryotic algae (Frischkorn et al., 2014; Wurch et al., 2019), this finding suggests that given enough ammonium, transporters are downregulated. Interestingly, glutarate-semialdehyde dehydrogenase (K00135, [EC:1.2.1.20], Fig 4 and 5, Table S4) displayed a unique, significant increase in transcript abundances in the ammonium + prey treatment, suggesting a potential accumulation of glutarate, a compound usually produced during biological catabolism of aromatic compounds (e.g. nicotinate and benzoate) and amino acids (e.g. L-lysine, L-hydroxylysine, and L-tryptophan) (Zhang et al., 2018). In addition, the up-regulation of glutaryl-CoA dehydrogenase (K00252, [EC:1.3.8.6], Fig 4 and 5, Table S4) and acetyl-CoA C-acetyltransferase (K00626, [EC:2.3.1.9], Fig 5, Table S6) suggests further degradation of glutarate to acetyl-CoA which can enter the citrate cycle for energy generation (Kurowska and Carroll, 1994; Rao et al., 2006; Wischgoll et al., 2009). While these genes (glutaryl-CoA dehydrogenase and acetyl-CoA C-acetyltransferase) showed no significant change in the ammonium only and nitrate treatment, they displayed significantly higher transcript abundances in the prey treatment, but glutarate-semialdehyde dehydrogenase was unaffected. Thus, the increase in glutarate was specific to heterotrophic nutrition and the degradation of amino acids.

Genes related to ubiquitin mediated proteolysis (K03349, K10578, K10587), RNA degradation (K12581, K12603), and protein processing in the endoplasmic reticulum (K01230, K09582, K10578, K23741) were in higher abundances (Table S6) in ammonium + prey treatment, suggesting the activation of protein catabolism (Myung et al., 2001; Wahl et al., 2009). While these genes were mostly unaltered in the prey treatment, the overall protein metabolism still indicated an activation of degradation enzymes involved in the extraction of N and energy from the prey. In addition, 2-acylglycerol O-acyltransferase 2 (K14457, [EC:2.3.1.22], Fig 4 and 5, Table S4) displayed higher transcript abundances in the ammonium + prey treatment indicating activation of the fatty acid degradation pathway. In fact, three other genes acetyl-CoA C-acetyltransferase (K00626, [EC:2.3.1.9]), glutaryl-CoA dehydrogenase (K00252, [EC:1.3.8.6]), and alcohol dehydrogenase 1/7 (K13951, [EC:1.1.1.1]) also had greater transcript abundances (Fig 4 and 5, Table S4, S6) while the fatty acid biosynthesis gene, S-malonyltransferase (K00645, [EC:2.3.1.39], Fig 5, Table S6) had lower transcript abundances, further evidencing the activation of fatty acid degradation (Li-Beisson et al., 2013) as also noted in the prey treatment. Similar to all other treatments, the glyoxylate pathway activation was observed in the ammonium + prey treatment by increased transcript abundances of malate synthase [EC:2.3.3.9], aconitate hydratase 2 / 2-methylisocitrate dehydratase [EC:4.2.1.3 4.2.1.99], and acetyl-CoA C-acetyltransferase [EC:2.3.1.9] (Fig 5 and Table S6) paralleling fatty acid degradation. Collectively the ammonium + prey treatment showed signs of both individual treatments: the assimilatory ammonium reduction was similar to that observed in the ammonium only treatment and the shift in protein metabolism and fatty acid metabolism towards that of catabolism was similar to the prey treatment. Overall, both the physiological and transcriptomic responses seen in the ammonium + prey treatment in comparison to the prey- or ammonium- only treatments, indicates that *D. acuminata* possessed the biochemical pathways to grow maximally as a mixotroph, consuming prey and ammonium.

4.7. Conclusion

Here, the physiological and transcriptomic responses elicited by differing nutritional sources were evident (Fig 5). *Dinophysis* was not able to grow when provided with nitrate, displaying a down regulation of multiple biochemical pathways and an overall starvation response in this treatment. Compared to the control and nitrate treatments, *Dinophysis* grew significantly faster when offered ammonium alone but slower than compared to ammonium + prey seemingly due to lack of key nutritional factors derived from prey that were necessary for photosynthesis (i.e. plastids). Similarly, *Dinophysis* feeding solely on *Mesodinium* grew significantly better than the control and nitrate treatments but was never significantly different from the ammonium only treatment. The ammonium only treatment grew phototrophically, while the prey only treatment utilized heterotrophic pathways associated with prey digestion and extracting nutrients from prey. Overall, the similarity of growth rates in the ammonium- and prey- only treatments suggested that the autotrophic and heterotrophic pathways associated with each treatment produce a similar amount of cellular energy. *Dinophysis* achieved maximal growth rates when offered ammonium + prey. Given that *Dinophysis* gets C and N from prey and C from photosynthesis, it would seem exogenous N is needed to balance the C acquired through photosynthesis as evidenced by the increase in N incorporation via the GO-GAT pathway and N recycling through amino acid degradation in the ammonium + prey treatment. *Dinophysis* growth on ammonium + prey was additive indicating that mixotrophy, using both autotrophic and heterotrophic pathways, while energetically expensive (Raven, 1997) was, nonetheless, optimal.

Declaration of Competing Interest

The authors declare no competing interests.

Acknowledgements

Partial support for this research was received from the National Oceanic and Atmospheric Administration National Centers for Coastal Ocean Science Competitive Research Program under awards NA17NOS4780184 and NA19NOS4780182 to CJG. This paper is ECOHAB publication number 987.

Supplementary materials

Supplementary material associated with this article can be found, in the online version, at doi:10.1016/j.hal.2021.102031.

References

Anderson, D.M., Burkholder, J.M., Cochlan, W.P., Glibert, P.M., Gobler, C.J., Heil, C.A., Kudela, R.M., Parsons, M.L., Rensel, J., Townsend, D.W., 2008. Harmful algal blooms and eutrophication: examining linkages from selected coastal regions of the United States. Harmful Algae 8 (1), 39–53.

Anderson, D.M., Cembella, A.D., Hallegraeff, G.M., 2012. Progress in understanding harmful algal blooms: paradigm shifts and new technologies for research, monitoring, and management. Ann. Rev. Mar. Sci. 4, 143–176.

Andrews, S., 2010. FastQC: a quality control tool for high throughput sequence data. Available online at: http://www.bioinformatics.babraham.ac.uk/projects/fastqc, version v0.11.5 ed.

Berges, J.A., Charlebois, D.O., Mauzerall, D.C., Falkowski, P.G., 1996. Differential effects of nitrogen limitation on photosynthetic efficiency of photosystems I and II in microalgae. Plant Physiol. 110 (2), 689.

Bi, Y., Wang, F., Zhang, W., 2019. Omics analysis for dinoflagellates biology research. Microorganisms 7 (9).

Bolger, A.M., Lohse, M., Usadel, B., 2014. Trimmomatic: a flexible trimmer for Illumina sequence data. Bioinformatics 30 (15), 2114–2120.

Bonachela, J.A., Raghib, M., Levin, S.A., 2011. Dynamic model of flexible phytoplankton nutrient uptake. Proc. Natl. Acad. Sci. 108 (51), 20633.

Bravo, I., Figueroa, R.I., 2014. Towards an ecological understanding of dinoflagellate cyst functions. Microorganisms 2 (1), 11–32.

Bray, N.L., Pimentel, H., Melsted, P., 2016. Near-optimal probabilistic RNA-seq Quantification. 34(5), 525–527.

Bryant, D.M., Johnson, K., DiTommaso, T., Tickle, T., Couger, M.B., Payzin-Dogru, D., Lee, T.J., Leigh, N.D., Kuo, T.H., Davis, F.G., Bateman, J., Bryant, S., Guzikowski, A. R., Tsai, S.L., Coyne, S., Ye, W.W., Freeman Jr., R.M., Peshkin, L., Tabin, C.J., Regev, A., Haas, B.J., Whited, J.L., 2017. A tissue-mapped axolotl de novo transcriptome enables identification of limb regeneration factors. Cell Rep 18 (3), 762–776.

Camacho, C., Coulouris, G., Avagyan, V., Ma, N., Papadopoulos, J., Bealer, K., Madden, T.L., 2009. BLAST+: architecture and applications. BMC Bioinformatic. 10 (1), 421.
Campbell, L., Olson, R.J., Sosik, H.M., Abraham, A., Henrichs, D.W., Hyatt, C.J., Buskey, E.J., 2010. First harmful *Dinophysis* (Dinophyceae, Dinophysiales) bloom in the U.S. is revealed by automated imaging flow cytometry. J. Phycol. 46 (1), 66–75.
Chen, F., Johns, M.R., 1991. Effect of C/N ratio and aeration on the fatty acid composition of heterotrophic *Chlorella sorokiniana*. J. Appl. Phycol. 3 (3), 203–209.
Collos, Y., Harrison, P.J., 2014. Acclimation and toxicity of high ammonium concentrations to unicellular algae. Mar. Pollut. Bull. 80 (1–2), 8–23.
Cooper, E.D., Bentlage, B., Gibbons, T.R., Bachvaroff, T.R., Delwiche, C.F., 2014. Metatranscriptome profiling of a harmful algal bloom. Harmful Algae 37, 75–83.
Deeds, J.R., Wiles, K., Heideman, G.B., White, K.D., Abraham, A., 2010. First US report of shellfish harvesting closures due to confirmed okadaic acid in Texas Gulf coast oysters. Toxicon 55 (6), 1138–1146.
DMF, M., 2015. Massachusetts Division of Marine Fisheries 2015 Annual Report. Dep. Fish Game. Massachusetts, p. 110 pgs.
Eddy, S.R., 2009. A new generation of homology search tools based on probabilistic inference. Genome informatics. Int. Conf. Genome Inf. 23 (1), 205–211.
Frischkorn, K.R., Harke, M.J., Gobler, C.J., Dyhrman, S.T., 2014. De novo assembly of *Aureococcus anophagefferens* transcriptomes reveals diverse responses to the low nutrient and low light conditions present during blooms. Front. Microbiol. 5, 375.
Fritz, L., Stringher, C.G., Colepicolo, P., 1996. Immunolocalization of nitrate reductase in the marine dinoflagellate *Gonyaulax polyedra* (Pyrrophyta). J. Phycol. 32 (4), 632–637.
García-Portela, M., Reguera, B., Gago, J., Gac, M.L., Rodríguez, F., 2020. Uptake of inorganic and organic nitrogen sources by *Dinophysis acuminata* and *D. acuta*. Microorganisms 8 (2), 187.
Glibert, P.M., Anderson, D.M., Gentien, P., Granéli, E., Sellner, K.G., 2005. The global, complex phenomena of harmful algal blooms. Oceanography 18 (2), 136–147.
Glibert, P.M., Lipschultz, F., McCarthy, J.J., Altabet, M.A., 1982. Isotope-dilution models of uptake and remineralization of ammonium by marine plankton. Limnol. Oceanogr. 27 (4), 639–650.
Grabherr, M.G., Haas, B.J., Yassour, M., Levin, J.Z., Thompson, D.A., Amit, I., Adiconis, X., Fan, L., Raychowdhury, R., Zeng, Q., Chen, Z., Mauceli, E., Hacohen, N., Gnirke, A., Rhind, N., di Palma, F., Birren, B.W., Nusbaum, C., Lindblad-Toh, K., Friedman, N., Regev, A., 2011. Full-length transcriptome assembly from RNA-Seq data without a reference genome. Nat. Biotechnol. 29 (7), 644–652.
Guillard, R.R., Ryther, J.H., 1962. Studies of marine planktonic diatoms. I. *Cyclotella nana* Hustedt, and *Detonula confervacea* Cleve. Can. J. Microbiol. 8 (2), 229–239.
Haas, B.J., Papanicolaou, A., Yassour, M., Grabherr, M., Blood, P.D., Bowden, J., Couger, M.B., Eccles, D., Li, B., Lieber, M., MacManes, M.D., Ott, M., Orvis, J., Pochet, N., Strozzi, F., Weeks, N., Westerman, R., William, T., Dewey, C.N., Henschel, R., LeDuc, R.D., Friedman, N., Regev, A., 2013. De novo transcript sequence reconstruction from RNA-seq using the Trinity platform for reference generation and analysis. Nat. Protoc. 8 (8), 1494–1512.
Hallegraeff, G.M., 1993. A review of harmful algal blooms and their apparent global increase. Phycologia 32 (2), 79–99.
Hallegraeff, G.M., 2010. Ocean climate change, phytoplankton community responses, and harmful algal blooms: a formidable predictive challenge. J. Phycol. 46 (2), 220–235.
Harke, M.J., Gobler, C.J., 2013. Global transcriptional responses of the toxic cyanobacterium, *Microcystis aeruginosa*, to nitrogen stress, phosphorus stress, and growth on organic matter. PLoS ONE 8 (7), e69834.
Harke, M.J., Gobler, C.J., 2015. Daily transcriptome changes reveal the role of nitrogen in controlling microcystin synthesis and nutrient transport in the toxic cyanobacterium, *Microcystis aeruginosa*. BMC Genomics 16 (1), 1068.
Hattenrath-Lehmann, T., Gobler, C.J., 2015. The contribution of inorganic and organic nutrients to the growth of a North American isolate of the mixotrophic dinoflagellate, *Dinophysis acuminata*. Limnol. Oceanogr. 60 (5), 1588–1603.
Hattenrath-Lehmann, T.K., Lusty, M.W., Wallace, R.B., Haynes, B., Wang, Z., Broadwater, M., Deeds, J.R., Morton, S.L., Hastback, W., Porter, L., Chytalo, K., Gobler, C.J., 2018. Evaluation of rapid, early warning approaches to track shellfish toxins associated with *Dinophysis* and *Alexandrium* blooms. Mar. Drugs 16 (1), 28.
Hattenrath-Lehmann, T.K., Marcoval, M.A., Berry, D.L., Fire, S., Wang, Z., Morton, S.L., Gobler, C.J., 2013. The emergence of *Dinophysis acuminata* blooms and DSP toxins in shellfish in New York waters. Harmful Algae 26 (0), 33–44.
Hattenrath-Lehmann, T.K., Marcoval, M.A., Mittlesdorf, H., Goleski, J.A., Wang, Z., Haynes, B., Morton, S.L., Gobler, C.J., 2015. Nitrogenous nutrients promote the growth and toxicity of *Dinophysis acuminata* during estuarine bloom events. PLoS ONE 10 (4), e0124148.
Heisler, J., Glibert, P.M., Burkholder, J.M., Anderson, D.M., Cochlan, W., Dennison, W. C., Dortch, Q., Gobler, C.J., Heil, C.A., Humphries, E., Lewitus, A., Magnien, R., Marshall, H.G., Sellner, K., Stockwell, D.A., Stoecker, D.K., Suddleson, M., 2008. Eutrophication and harmful algal blooms: a scientific consensus. Harmful Algae 8 (1), 3–13.
Ikaran, Z., 2015. The effect of nitrogen limitation on the physiology and metabolism of *Chlorella vulgaris* var L3. Algal Res. v 10, pp. 134-144-2015 v.2010.
Illumina, 2000, 16S metagenomic library prep guide. https://support.illumina.com/documents/documentation/chemistry_documentation/16s/16s-metagenomic-library-prep-guide-15044223-b.pdf.
Ji, N., Lin, L., Li, L., Yu, L., Zhang, Y., Luo, H., Li, M., Shi, X., Wang, D.-Z., Lin, S., 2018. Metatranscriptome analysis reveals environmental and diel regulation of a *Heterosigma akashiwo* (raphidophyceae) bloom. Environ. Microbiol. 20 (3), 1078–1094.
Jitrapakdee, S., St Maurice, M., Rayment, I., Cleland, W.W., Wallace, John C., Attwood, Paul V., 2008. Structure, mechanism and regulation of pyruvate carboxylase. Biochem. J. 413 (3), 369–387.
Jones, P., Binns, D., Chang, H.-Y., Fraser, M., Li, W., McAnulla, C., McWilliam, H., Maslen, J., Mitchell, A., Nuka, G., Pesseat, S., Quinn, A.F., Sangrador-Vegas, A., Scheremetjew, M., Yong, S.-Y., Lopez, R., Hunter, S., 2014. InterProScan 5: genome-scale protein function classification. Bioinformatics 30 (9), 1236–1240.
Kanehisa, M., Sato, Y., Morishima, K., 2016. BlastKOALA and GhostKOALA: KEGG tools for functional characterization of genome and metagenome sequences. J. Mol. Biol. 428 (4), 726–731.
Kim, S., Kang, Y.G., Kim, H.S., Yih, W., Coats, D.W., Park, M.G., 2008. Growth and grazing responses of the mixotrophic dinoflagellate *Dinophysis acuminata* as functions of light intensity and prey concentration. Aquat. Microb. Ecol. 51 (3), 301–310.
Kissing, S., Hermsen, C., Repnik, U., Nesset, C.K., von Bargen, K., Griffiths, G., Ichihara, A., Lee, B.S., Schwake, M., De Brabander, J., Haas, A., Saftig, P., 2015. Vacuolar ATPase in phagosome-lysosome fusion. J. Biol. Chem. 290 (22), 14166–14180.
Kudela, R., Seeyave, S., Cochlan, W., 2010a. The role of nutrients in regulation and promotion of harmful algal blooms in upwelling systems. Prog. Oceanogr. 85 (1), 122–135.
Kudela, R.M., Howard, M.D.A., Jenkins, B.D., Miller, P.E., Smith, G.J., 2010b. Using the molecular toolbox to compare harmful algal blooms in upwelling systems. Prog. Oceanogr. 85 (1), 108–121.
Kudela, R.M., Lane, J.Q., Cochlan, W.P., 2008. The potential role of anthropogenically derived nitrogen in the growth of harmful algae in California, USA. Harmful Algae 8 (1), 103–110.
Kurowska, E.M., Carroll, K.K., 1994. Hypercholesterolemic responses in rabbits to selected groups of dietary essential amino acids. J. Nutr. 124 (3), 364–370.
Lee, S., Kang, Y.C., Fuhrman, J.A., 1995. Imperfect retention of natural bacterioplankton cells by glass-fiber filters. Mar. Ecol. Prog. Ser. 119 (1–3), 285–290.
Li-Beisson, Y., Shorrosh, B., Beisson, F., Andersson, M.X., Arondel, V., Bates, P.D., Baud, S., Bird, D., DeBono, A., Durrett, T.P., Franke, R.B., Graham, I.A., Katayama, K., Kelly, A.A., Larson, T., Markham, J.E., Miquel, M., Molina, I., Nishida, I., Rowland, O., Samuels, L., Schmid, K.M., Wada, H., Welti, R., Xu, C., Zallot, R., Ohlrogge, J., 2013. Acyl-Lipid Metabolism. Arabidopsis Book, 2013(11).
Lie, A.A.Y., Liu, Z., Terrado, R., Tatters, A.O., Heidelberg, K.B., Caron, D.A., 2017. Effect of light and prey availability on gene expression of the mixotrophic chrysophyte, *Ochromonas* sp. BMC Genomics 18 (1), 163.
Lie, A.A.Y., Liu, Z., Terrado, R., Tatters, A.O., Heidelberg, K.B., Caron, D.A., 2018. A tale of two mixotrophic chrysophytes: insights into the metabolisms of two *Ochromonas* species (Chrysophyceae) through a comparison of gene expression. PLoS ONE 13 (2), e0192439.
Lin, S., 2011. Genomic understanding of dinoflagellates. Res. Microbiol. 162 (6), 551–569.
Lin, S.J., Zhang, H., Spencer, D.F., Norman, J.E., Gray, M.W., 2002. Widespread and extensive editing of mitochondrial mRNAs in dinoflagellates. J. Mol. Biol. 320, 727–739.
Lloyd, J.K., Duchin, J.S., Borchert, J., Quintana, H.F., Robertson, A., 2013. Diarrhetic Shellfish Poisoning, Washington, USA, 2011. Emerg. Infect. Dis. 19 (8), 1314–1316.
Luo, H., Lin, X., Li, L., Lin, L., Zhang, C., Lin, S., 2017. Transcriptomic and physiological analyses of the dinoflagellate *Karenia mikimotoi* reveal non-alkaline phosphatase-based molecular machinery of ATP utilisation. Environ. Microbiol. 19 (11), 4506–4518.
Maestrini, S.Y., Berland, B.R., Grzebyk, D., Spano, A.M., 1995. *Dinophysis* spp cells concentrated from nature for experimental purposes, using size fractionation and reverse migration. Aquat. Microb. Ecol. 9 (2), 177–182.
Medlin, L., 2013. Molecular tools for monitoring harmful algal blooms. Environ. Sci. Pollut. Res. 20 (10), 6683–6685.
Medlin, L.K., Orozco, J., 2017. Molecular techniques for the detection of organisms in aquatic environments, with emphasis on harmful algal bloom species. Sensors (Basel) 17 (5), 1184.
Montoya, J.P., Voss, M., Kahler, P., Capone, D.G., 1996. A simple, high-precision, high-sensitivity tracer assay for N_2 fixation. Appl. Environ. Microbiol. 62 (3), 986–993.
Morey, J.S., Monroe, E.A., Kinney, A.L., Beal, M., Johnson, J.G., Hitchcock, G.L., Van Dolah, F.M., 2011. Transcriptomic response of the red tide dinoflagellate, *Karenia brevis*, to nitrogen and phosphorus depletion and addition. BMC Genomics 12 (1), 346.
Myung, J., Kim, K.B., Crews, C.M., 2001. The ubiquitin-proteasome pathway and proteasome inhibitors. Med. Res. Rev. 21 (4), 245–273.
Neuhauser, W., Haltrich, D., Kulbe, K.D., Nidetzky, B., 1997. NAD(P)H-dependent aldose reductase from the xylose-assimilating yeast *Candida tenuis*. Isolation, characterization and biochemical properties of the enzyme. Biochem. J. 326, 683–692.
Nielsen, L.T., Krock, B., Hansen, P.J., 2013. Production and excretion of okadaic acid, pectenotoxin-2 and a novel dinophysistoxin from the DSP-causing marine dinoflagellate *Dinophysis acuta* - Effects of light, food availability and growth phase. Harmful Algae 23, 34–45.
Orcutt, K.M., Lipschultz, F., Gundersen, K., Arimoto, R., Michaels, A.F., Knap, A.H., Gallon, J.R., 2001. A seasonal study of the significance of N_2 fixation by *Trichodesmium* spp. at the Bermuda Atlantic Time-series Study (BATS) site. Deep-Sea Res. Part Ii-Top. Stud. Oceanogr. 48 (8–9), 1583–1608.
Park, M.G., Kim, S., Kim, H.S., Myung, G., Kang, Y.G., Yih, W., 2006. First successful culture of the marine dinoflagellate *Dinophysis acuminata*. Aquat. Microb. Ecol. 45 (2), 101–106.

Peacock, M.B., Gibble, C.M., Senn, D.B., Cloern, J.E., Kudela, R.M., 2018. Blurred lines: multiple freshwater and marine algal toxins at the land-sea interface of San Francisco Bay, California. Harmful Algae 73, 138–147.
Pimentel, H., Bray, N.L., Puente, S., Melsted, P., Pachter, L., 2017. Differential analysis of RNA-seq incorporating quantification uncertainty. Nat. Methods 14 (7), 687–690.
Quast, C., Pruesse, E., Yilmaz, P., Gerken, J., Schweer, T., Yarza, P., Peplies, J., Glöckner, F.O., 2012. The SILVA ribosomal RNA gene database project: improved data processing and web-based tools. Nucleic Acids Res. 41 (D1), D590–D596.
Raho, N., Pizarro, G., Escalera, L., Reguera, B., Marin, I., 2008. Morphology, toxin composition and molecular analysis of *Dinophysis ovum* Schutt, a dinoflagellate of the "*Dinophysis acuminata* complex". Harmful Algae 7 (6), 839–848.
Rao, K.S., Albro, M., Dwyer, T.M., Frerman, F.E., 2006. Kinetic mechanism of glutaryl-CoA dehydrogenase. Biochemistry 45 (51), 15853–15861.
Raven, J., 1997. Phagotrophy in phototrophs. Limnol. Oceanogr. 42 (1), 198–205.
Reguera, B., Riobó, P., Rodríguez, F., Díaz, P., Pizarro, G., Paz, B., Franco, J., Blanco, J., 2014. *Dinophysis* toxins: causative organisms, distribution and fate in shellfish. Mar. Drugs 12 (1), 394–461.
Reguera, B., Velo-Suarez, L., Raine, R., Park, M.G., 2012. Harmful *Dinophysis* species: a review. Harmful Algae 14, 87–106.
Riisgaard, K., Hansen, P.J., 2009. Role of food uptake for photosynthesis, growth and survival of the mixotrophic dinoflagellate *Dinophysis acuminata*. Mar. Ecol. Prog. Ser. 381, 51–62.
Rubin, E.T., Cheng, S., Montalbano, A.L., Menden-Deuer, S., Rynearson, T.A., 2019. Transcriptomic response to feeding and starvation in a herbivorous dinoflagellate. Front. Mar. Sci. 6 (246).
Ryan, D.E., Pepper, A.E., Campbell, L., 2014. De novo assembly and characterization of the transcriptome of the toxic dinoflagellate *Karenia brevis*. BMC Genomics. 15 (1), 888.
Sampayo, M.A.D., 1993. Trying to cultivate *Dinophysis* spp. In: Smayda, T., Shimizu, Y. (Eds.), Toxic Phytoplankton Blooms in the Sea. Elsevier, Amsterdam, pp. 807–810.
Seeyave, S., Probyn, T.A., Pitcher, G.C., Lucas, M.I., Purdie, D.A., 2009. Nitrogen nutrition in assemblages dominated by *Pseudo-nitzschia* spp., *Alexandrium catenella* and *Dinophysis acuminata* off the west coast of South Africa. Mar. Ecol. Prog. Ser. 379, 91–107.
Shi, X., Lin, X., Li, L., Li, M., Palenik, B., Lin, S., 2017. Transcriptomic and microRNAomic profiling reveals multi-faceted mechanisms to cope with phosphate stress in a dinoflagellate. ISME J. 11 (10), 2209–2218.
Shultz, D., Campbell, L., Kudela, R.M., 2019. Trends in *Dinophysis* abundance and diarrhetic shellfish toxin levels in California mussels (*Mytilus californianus*) from Monterey Bay, California. Harmful Algae 88, 101641.
Smayda, T.J., 1997. Harmful algal blooms: their ecophysiology and general relevance to phytoplankton blooms in the sea. Limnol. Oceanogr. 42 (5), 1137–1153.
Stüken, A., Orr, R.J., Kellmann, R., Murray, S.A., Neilan, B.A., Jakobsen, K.S., 2011. Discovery of nuclear-encoded genes for the neurotoxin saxitoxin in dinoflagellates. PLoS ONE 6 (5), e20096.
Swanson, K.M., Flewelling, L.J., Byrd, M., Nunez, A., Villareal, T.A., 2010. The 2008 Texas *Dinophysis ovum* bloom: distribution and toxicity. Harmful Algae 9 (2), 190–199.
Tong, M., Smith, J., Kulis, D., Anderson, D., 2015. Role of dissolved nitrate and phosphate in isolates of *Mesodinium rubrum* and toxin-producing *Dinophysis acuminata*. Aquat. Microb. Ecol. 75 (2), 169–185.
Trainer, V., Moore, L., Bill, B., Adams, N., Harrington, N., Borchert, J., da Silva, D., Eberhart, B.-.T., 2013. Diarrhetic shellfish toxins and other lipophilic toxins of human health concern in Washington State. Mar Drugs 11 (6), 1815–1835.
Van Dolah, F.M., 2000. Marine algal toxins: origins, health effects, and their increased occurrence. Environ. Health Perspect. 108, 133–141.
Wahl, M.C., Will, C.L., Lührmann, R., 2009. The spliceosome: design principles of a dynamic RNP machine. Cell 136 (4), 701–718.
Werner, A.K., Witte, C.-.P., 2011. The biochemistry of nitrogen mobilization: purine ring catabolism. Trends Plant Sci. 16 (7), 381–387.
Williams, E., Place, A., Bachvaroff, T., 2017. Transcriptome analysis of core dinoflagellates reveals a universal bias towards "GC" rich codons. Mar. Drugs 15 (5), 125.
Wischgoll, S., Taubert, M., Peters, F., Jehmlich, N., von Bergen, M., Boll, M., 2009. Decarboxylating and nondecarboxylating glutaryl-coenzyme a dehydrogenases in the aromatic metabolism of obligately anaerobic bacteria. J. Bacteriol. 191 (13), 4401.
Wisecaver, J.H., Hackett, J.D., 2010. Transcriptome analysis reveals nuclear-encoded proteins for the maintenance of temporary plastids in the dinoflagellate *Dinophysis acuminata*. BMC Genomics 11.
Wolny, J.L., Egerton, T.A., Handy, S.M., Stutts, W.L., Smith, J.L., Whereat, E.B., Bachvaroff, T.R., Henrichs, D.W., Campbell, L., Deeds, J.R., 2020. Characterization of *Dinophysis* spp. (Dinophyceae, Dinophysiales) from the mid-Atlantic region of the United States. J. Phycol. 56 (2), 404–424.
Wood, D.E., Salzberg, S.L., 2014. Kraken: ultrafast metagenomic sequence classification using exact alignments. Genome Biol. 15 (3), R46.
Wurch, L.L., Alexander, H., Frischkorn, K.R., Haley, S.T., Gobler, C.J., Dyhrman, S.T., 2019. Transcriptional shifts highlight the role of nutrients in harmful brown tide dynamics. Front. Microbiol. 10 (136).
Wurch, L.L., Haley, S.T., Orchard, E.D., Gobler, C.J., Dyhrman, S.T., 2011. Nutrient-regulated transcriptional responses in the brown tide-forming alga *Aureococcus anophagefferens*. Environ. Microbiol. 13 (2), 468–481.
Zhang, H., Hou, Y., Miranda, L., Campbell, D.A., Sturm, N.R., Gaasterland, T., Lin, S., 2007. Spliced leader RNA trans-splicing in dinoflagellates. Proc. Natl. Acad. Sci. 104 (11), 4618–4623.
Zhang, M., Gao, C., Guo, X., Guo, S., Kang, Z., Xiao, D., Yan, J., Tao, F., Zhang, W., Dong, W., Liu, P., Yang, C., Ma, C., Xu, P., 2018. Increased glutarate production by blocking the glutaryl-CoA dehydrogenation pathway and a catabolic pathway involving L-2-hydroxyglutarate. Nat. Commun. 9 (1), 2114.
Zhang, Y., Lin, X., Shi, X., Lin, L., Luo, H., Li, L., Lin, S., 2019. Metatranscriptomic signatures associated with phytoplankton regime shift from diatom dominance to a dinoflagellate bloom. Front. Microbiol. 10 (590).
Zhuang, Y., Zhang, H., Hannick, L., Lin, S., 2015. Metatranscriptome profiling reveals versatile N-nutrient utilization, CO_2 limitation, oxidative stress, and active toxin production in an *Alexandrium fundyense* bloom. Harmful Algae 42, 60–70.